DR. YOULI HU (Orcid ID : 0000-0001-5507-6123)

Article type : Research Report

Extracelluar matrix protein anosmin-1 modulates olfactory ensheathing cell maturation in chick olfactory bulb development

Running title: Anosmin-1 and olfactory ensheathing cell

Youli Hu[§, 1,2], Thomas Butts[3,4], Subathra Poopalasundaram[3], Anthony Graham[3] and Pierre-Marc Bouloux[2]

[1] Department of Anesthesiology, the First Affiliated Hospital of Nanjing Medical University/Jiangsu Province Hospital, Nanjing, China, 210029

[2] Centre for Neuroendocrinology, UCL Medical School, Royal Free Campus, London NW3 2PF，UK

[3] Centre for Developmental Neurobiology, King's College London, London SE1 1UL，UK

[4] School of Life Sciences and Department of Cellular and Molecular Physiology, University of Liverpool, Liverpool, L69 7ZH，UK

§Address correspondence to: Youli Hu, Centre for Neuroendocrinology, UCL Medical School, Royal Free Campus, London NW3 2PF， UK. Tel. 44-20-7794 0500 ext:38158; Fax: 44-20-7317 7625; E-mail: huyouli@hotmail.com

This article has been accepted for publication and undergone full peer review but has not been through the copyediting, typesetting, pagination and proofreading process, which may lead to differences between this version and the Version of Record. Please cite this article as doi: 10.1111/ejn.14483

Funding information

Grant sponsor: This work was supported by National Natural Science Foundation of China (NSFC) (81571193)

Key words: Kallmann syndrome, astrocyte, fibroblast growth factor receptor， embryo

Author contributions：Y Hu designed study, performed the experiments, analysed data and drafted paper; T Butts and S Poopalasundaram performed the experiments and analysed data; A Graham and PM Bouloux drafted paper.

Abstract

Olfactory ensheathing cells (OECs) are a specialized class of glia, wrapping around olfactory sensory axons that target the olfactory bulb (OB) and cross the peripheral nervous system / central nervous system boundary during development and continue to do so post-natally. OEC subpopulations perform distinct subtype-specific functions dependent on their maturity status. Disrupted OEC development is thought to be associated with abnormal OB morphogenesis, leading to anosmia, a defining characteristic of Kallmann syndrome. Hence, anosmin-1 encoded by Kallmann syndrome gene (*KAL-1*) might modulate OEC differentiation/maturation in the OB. We performed *in ovo* electroporation of shRNA in the olfactory placode to knock down *kal* in chick embryos, resulting in abnormal OB morphogenesis and loss of olfactory sensory axonal innervation into OB. BLBP expressing OECs appeared to form a thinner and poorly organized outmost OB layer where SOX10 expressing OECs were completely absent with emergence of GFAP expressing OECs. Furthermore, in embryonic day 10 chick OB explant cultures, GFAP expression in OECs accumulating along the OB nerve layers was dramatically reduced by recombinant anosmin-1. We then purified immature OECs from embryonic day 10 chick OB. These cells express GFAP after 7 days *in vitro*, exhibiting a multipolar morphology. Over-expression of chick anosmin, exogenous anosmin-1 or FGF2 could inhibit GFAP expression with cells presenting elongated morphology, which was blocked by the FGF receptor inhibitor Su5402. These data demonstrate that anosmin-1 functions via FGF signalling in regulating OEC maturation,

thereby providing a permissive glial environment for axonal innervation into the OB during development.

1 INTRODUCTION

Olfactory sensory neurons, whether after damage or as part of normal cell turnover, continually extend axons from the olfactory epithelium, through the lamina propria to enter the outer layer of the olfactory bulb (OB) (Farbman, 1990;Graziadei and Graziadei, 1979). In the OB, they form synapses with the dendrites of mitral/tufted cells establishing glomeruli-like structures. This property depends on the specialised glial cells in the olfactory system, so-called olfactory ensheathing cells (OECs) (Schwob, 2002). OECs originate from the neural crest (Barraud et al., 2010) and wrap around olfactory sensory axons migrating towards the anterior forebrain where they, along with olfactory axons, form the olfactory nerve layer (ONL) of the OB. It has been proposed that OECs may exhibit the unique property of maintaining continuous open channels, permitting ingress of olfactory nerve fibres into the bulb (Li et al., 2005; Williams et al., 2004). Moreover, cross-talk between astrocytes and OECs are believed to underpin the mechanism of continuous neuronal re-innervation, as OECs interweave with astrocytes within the deeper ONL(Doucette, 1991;Li et al., 2005;Raisman, 1985).

In the developing ONL of the OB, two OEC subpopulations, from different stages of maturation and evincing different antigenic profiles, exert distinct functions during olfactory axonal outgrowth and targeting to specific glomeruli. Thus, p75 and GFAP OEC expression in the outer region of ONL are thought to characterize a more mature OEC population for olfactory axon outgrowth and OB targeting, whereas NPY and Runx1 positive OEC subpopulations from the inner ONL are thought to function as more immature OECs influencing axonal sorting and specific synapse formation (Astic et al., 1998;Murthy et al., 2014). Furthermore, transcription factor SOX10 positive OEC subpopulations play a role in fasciculation and targeting of the olfactory nerve fibers into the OB for ONL organization (Pingault et al., 2013).

In humans, spontaneous mutations of the neural crest OEC marker SOX10 have recently been described in Kallmann syndrome (KS) patients, the development disorder characterised by abnormal OB morphogenesis and delayed puberty due to disrupted migration of gonadotropin-releasing hormone (GnRH) neurons along with the olfactory,

vomeronasal, and terminal nerves (Barraud et al., 2013;Pingault et al., 2013). Recent study demonstrated that OEC maturation is involved in neurite outgrowth of GnRH neurons during migration (Geller et al., 2017). These findings possibly link the OEC development with the aetiology of KS.

Loss of function of extracellular matrix protein anosmin-1, encoded by the X-linked *KAL-1* gene, is almost invariably associated with a highly penetrant phenotype with abnormal sense of smell, frequently resulting from OB dysgenesis. Immunohistochemical study of two *KAL-1*-deleted or mutated human foetuses (aged 19 and 25 weeks) revealed that axons of olfactory sensory neurons could not penetrate into the forebrain, failing to establish synaptic connection within the OB (Schwanzel-Fukuda et al., 1989; Teixeira et al., 2010). During human embryogenesis, anosmin-1 is expressed in the interneurons and ONL of the developing OB, and has been shown to demonstrate chemoattractive and stimulative properties on axonal branching, neurite outgrowth and neuronal migration (Gonzalez-Martinez et al., 2004; Hu et al., 2004; Hu et al., 2009; Legouis et al., 1993; Lutz et al., 1994; Soussi-Yanicostas et al., 1998). More recent evidence, however, suggests that anosmin-1 may also modulate glial cell development. Thus, anosmin-1 actions within the neural crest, the site of origin of OECs, may result from its effect in enhancing FGF8 activity while inhibiting BMP5 and Wnt3a signalling (Endo et al., 2012). Furthermore, as the migration of OEC from the olfactory placode towards the telencephalon occurs before *KAL-1* expression in the presumptive OB, suggesting that anosmin-1 does not appear essential for initial OEC migration. Based on these observations, we hypothesized that anosmin-1 might modulate OEC maturation, enabling the establishment of stable synaptic connections between olfactory sensory axons and the OB anlage during embryogenesis.

In the present study, we have performed *in ovo* electroporation of shRNA in the olfactory placode to knock down *kal* function in chick embryos to further elucidate the mode of action of anosmin-1 in OB morphogenesis, and demonstrate its function in the development and maturation of OECs. Moreover, in OB explants and *in vitro* OB dissociated cell cultures, exogenous anosmin-1 down-regulated GFAP expression in OEC via an interaction with FGF signalling. Our data provide a novel mechanistic link between loss of function mutations in anosmin-1 in humans and the resulting severe anosmia.

2 MATERIALS AND METHODS

2.1 Plasmids used for *in ovo* electroporation

Three 21-nucleotide long sequences, within the chicken *kal* cDNA (NM_205424) were selected to generate shRNA and designed by GenScript (GenScript USA Inc.) to knock down chicken anosmin. Selected shRNAs were cloned into the miRNA site of the pRFP-C-RS vector (kindly provided by Professor Uwe Drescher, King's College London). To evaluate their efficiency, CHO cells were transfected with a chicken 6xHis tagged anosmin expression construct (*kal* in pCAGGS, kindly provided by Ken Yamada, NIH) and each shRNA, including the empty vector or scrambled shRNA were used as controls. Cells were cultured for 2 days, and processed for Western blot analysis using antibodies to chicken anosmin (kindly provided by Ken Yamada, NIH) and β-actin (Sigma). The optical density of the specific band was quantified and silencing, relative to β-actin for each individual sample, calculated. Finally general silencing was calculated relative to the control (pRFP-C-RF vector alone). Optimal silencing was obtained with kal shRNA-2 (>95%, sequence: CGGACTGGTAGATCCTTACCT). Percentage silencing was calculated from three independent experiments. This construct was chosen for *in ovo* electroporation to knock down *kal* in chick. No effect was seen when cells were transfected with scrambled control shRNA.

2.2 *In ovo* electroporation

The stage of chick embryos used in this study is within half the gestation period [embryonic day (E) 11] and is approved under the Animals (Scientific Procedures) Act 1986. Fertilized hens' eggs (Henry Stewart Farm) were incubated at 38 °C to Hamburger–Hamilton (HH) stage 11–12 (E2) and processed for electroporation. kal shRNA constructs or scrambled shRNA at concentrations of 0.8 or 2mg/mL were microinjected into the midbrain to avoid artificial damage on the anterior forebrain and then current was applied across the midbrain and one side of olfactory placode, using physical positioning of electrodes. Upon application of the electric current, kal shRNA construct was electroporated into cells on the same side of the olfactory placode as the anode, since DNA is negatively charged, and generates an internal negative, unmodified control on the non-electroporated side. After applying five 4.0–4.2V pulses, 50ms each, at 500-ms intervals with the electroporator (CUY21SC, NEPA

GENE CO., LTD), eggs were sealed and incubated to E10. Embryos were harvested and the whole brain was dissected in 0.1 M PBS, fixed overnight in 4% (w/v) paraformaldehyde in PBS (PFA) for immunostaining and *in situ* hybridization as described below.

2.3 E10 OB explant cultures

OBs from E10 chick embryos were dissected, immobilized in collagen gel and cultured in F12 supplemented with N2 (Gibco). OB explants were cultured for 2h (control, n=9), treated with (n=15)/without 5nM recombinant anosmin-1 (n=20) for 3 days *in vitro* (DIV), and fixed with 4% (w/v) formaldehyde in PBS for 1 hour followed by fixation with MEMFA (10% (v/v) MEM salts and 10% (v/v) formaldehyde) for 2 hours.

2.4 Primary cultures of OB glial cells

E10 OBs were digested with 0.05% (v/v) trypsin for 25 minutes at 37^{o}C and rinsed twice with DMEM/F12 medium (ABM). ABM with 10% (v/v) FBS (AGM) and 10% (w/v) BSA were added and trituration repeated to dissociate cells. 4% (w/v) BSA was gently layered under the cell suspension to create a distinct interface, spun for 15 minutes at 500g in a cooled centrifuge at 4^{o}C, and the cell pellet re-suspended in AGM. Approximately 7X10^{6} cells were plated in AGM for 2 weeks until the cells had grown to complete confluence. After shaking the flask at 250 rpm to remove neurons and microglia, the media was removed and cells were rinsed twice with 10 ml ABM, followed by incubation with 0.1% (v/v) trypsin for 3-4 min. Cells were re-suspended with AGM and centrifuged at 400g for 15 minutes. The cells were washed three times with ABM. OB glial cells were then plated at a density of 2X10^{5} cells in ADM (AGM+0.5xG5 supplement, Gibco) into 6-well plates containing 0.05mg/ml poly-D-Lys coated cover-slips. In one experiment, cells were treated with 5nM anosmin-1, 2nM FGF2 and 5nM anosmin-1 plus 20μM Su5402 (FGFR inhibitor) or 2nM FGF2 for 7 days in culture, fixed in PFA. In another experiment for expression of anosmin, primary OB cells were transfected with 1μg *kal*-pCAGGS construct or empty vector with FuGene6 in serum-free medium. After incubation for 48 hours, cells were fixed for immunostaining or lysed for Western blotting to detect GFAP expression. The GFAP band and fluorescence intensities were measured using the Software Image J (National Institutes of Health, Bethesda, MD). The relative GFAP band to actin ratio was calculated and all relative GFAP intensities were then compared with the control sample (vector only or no treatment group, 100%). The statistical significance was calculated using paired Student's t test (n=3).

2.5 Transcription of DIG-labelled RNA probes

RNA probe for *in situ* hybridisation was generated by PCR amplification using specific primers for chick *kal* (forward: AACACGCTGGGGTCAGATAC and reverse: TGGAGGAAGGTCAGGTGTTC) and cloned into pGEM-T Easy vector (Promega). RNA probes were transcribed using either the T7 or SP6 RNA polymerase on linearised DNA template and then purified using Microspin G-50 columns (GE Healthcare), according to the manufacturer's instructions and stored at -20°C until required.

2.6 Whole mount RNA *in situ* hybridisation

In situ hybridisation was carried out as described previously (Nieto et al., 1996). Briefly, Six E10 embryos from vector only and scrambled shRNA group as well as three E10 embryos from shRNA-2 group were dissected and fixed overnight in PFA, dehydrated in methanol, bleached in H_2O_2 and rehydrated. Incisions were made in the hindbrain of embryos to prevent probe from being trapped, known to result in high background and non-specific staining. Embryos were permeabilised with two 20 minute detergent mix (1% (v/v) IGEPAL, 1% (w/v) SDS, 0.5% (w/v) deoxycholate, 50mM Tris-HCl, pH8.0, 1mM EDTA, 150mM NaCl) washes, and fixed again in PFA. Embryos were transferred into pre-hybridisation buffer (50% (v/v) formamide, 5X SSC (pH4.5), 2% (w/v) SDS and 20% (w/v) blocking reagent (Roche)) for 1 hour at 70°C. Hybridisation was carried out at 70°C overnight, in fresh pre-hybridisation buffer containing 1µg/ml DIG-labelled RNA probe.

Embryos were rinsed twice in Solution X (50% (v/v) formamide, 2X SSC (pH4.5) and 1% (w/v) SDS), followed by two 30 minute washes at 70°C. They were then rinsed three or more times in MABT (100mM maleic acid, 150mM NaCl and 1% (v/v) Tween-20), and left in MABT for 30 minutes. Embryos were transferred into blocking solution (2% (w/v) blocking reagent, 20% (v/v) goat serum in MABT, and rocked for 1-2 hours at room temperature. Anti-DIG antibody (AP-conjugate; Roche) binding was carried out at a dilution of 1:2000 in fresh blocking solution, at 4°C overnight on a shaker.

Embryos were then washed and equilibrated in NTMT (100mM NaCl, 100mM Tris-HCl (pH9.5), 50mM MgCl2 and 1% (v/v) Tween-20) for 10 minutes each. The colour reaction was carried out in NTMT, using NBT/BCIP at 5µl/ml as the chromogenic substrate. The colour reaction was permanently terminated by washing embryos in PBST, and then embryos were re-fixed in PFA.

2.7 Immunostaining

For cryosectioning, E10 OB explants and electroporated E10 OBs were cryoprotected in 20-30% (w/v) sucrose in PBS, embedded in O.C.T and frozen on dry-ice. Approximately 20 cryosections were cut on a cryostat (10μm) and mounted directly onto subbed slides. Electroporated E10 OBs were paraffin sectioned for haemotoxylin and eosin (H&E) staining and βIII-tubulin immunostaining.

Explant cultures, tissue sections and primary cultured OB cells were washed in PBS containing 1% (v/v) Triton X-100, blocked with 10% (v/v) goat serum in PBS containing 1% (v/v) Triton X-100 and incubated with specific primary antibodies for GFAP (1:250, Sigma), BLBP (1:250, cell signalling), Sox10 (1:1000, gift from Dr. Silvana Guioli, National Institute for Medical Research, UK), βIII-tubulin (1:500, ab18207, Abcam), Transitin (the avian homologue of nestin, 1:100, Developmental Studies Hybridoma Bank, DSHB) and Vimentin (1:50, Sigma). After washing in PBS containing 1% (v/v) Triton X-100, samples were incubated with Alexa Fluor 488 or 594 goat anti-mouse or anti-rabbit IgG (Invitrogen). Images were acquired using an epifluorescence microscope.

2.8 RT-PCR

Total mRNA was extracted with Trizol from purified OB immature glial cells and reverse transcribed with Superscript II RT kit (Invitrogen). Specific primers were designed to amplify genes including *kal*, *fgfr1-3* b and c isoforms (Appendix: Supplemental data 1).

3 RESULTS

3.1 *In vivo* knock down of *kal* results in abnormal OB development

To gain insights into the potential role of chick anosmin in OB development, we electroporated chicken embryos with RFP-fluorescently tagged shRNA constructs to knock down *kal* expression, using scrambled shRNA as control. We first evaluated the efficiency of shRNA to silence *kal* by co-transfecting CHO cells with the chick *kal* expression vector and scrambled shRNA, or with the three designed kal shRNAs (Fig. 1a). All of the three kal shRNAs showed significant inhibition of *kal* gene expression, with optimal silencing obtained for kal shRNA-2; this was subsequently used for *in ovo* electroporation experiments.

We further examined whether kal shRNA-2 could effectively knock down endogenous *kal* by *in situ* hybridization. E2 chick embryos were electroporated with vector only, scrambled shRNA or 2mg/ml shRNAs respectively (Fig. 1b). After further incubation to E10, embryos were processed for *in situ* hybridization with a specific *kal* riboprobe. *Kal* transcripts were specifically detected in OBs electroporated with vector only and confined to a distinct band that coincides with the mitral cell layer (Fig. 1b I), which is consistent with the previously described *kal* expression profile in chicken (Legouis et al., 1993;Lutz et al., 1994). Control hybridizations with sense riboprobes gave no signal (Fig. 1b II). Distinct bands of *kal* expression close to the outmost layer of OB were also observed in both normal developed OBs with scrambled shRNA transfection (Fig. 1b III). By contrast, *kal* expression was absent on one side of kal shRNA-2 electroporated embryos without OB formation (Fig. 1b IV, double arrow), while present on the contralateral side with a normal OB (Fig. 1b IV, single arrow).

3.2 Dose-relevant effects of *kal* knock down on OB morphogenesis

To further investigate the specificity and dose-relevant effect of kal shRNA-2, chick embryos were electroporated at E2 with shRNA constructs at different concentrations and then processed to visualise RFP at E10 (Fig. 2). The transfected forebrains usually displayed much higher RFP expression, in one OB up to E10 stage. It was observed that scrambled construct and low (0.8mg/ml) kal siRNA-2 concentrations resulted in normal OB morphogenesis, even on the OB side with stronger RFP expression (Fig. 2a and b). However, *kal* knockdown, effected by increasing kal shRNA-2 to 2mg/ml resulted in striking and reproducible olfactory system defects, including OB hypoplasia and primary failure of olfactory sensory axons to reach the forebrain. Such hypoplastic OBs generally had much higher RFP expression, indicating greater *kal* transcription inhibition; by contrast, the contralateral side without RFP expressing had morphologically normal OB (Fig. 2c). The general morphology of the whole forebrain was similar on both sides, indicating a specific function of *kal* on OB differentiation and evagination from the anterior forebrain. These morphological defects induced by chicken *kal* knock down closely resemble the histopathological observations of human individuals affected by the loss of function of *KAL-1* in X-KS patients. Furthermore, human anosmin-1 when mutated in X-KS cause an extremely high prevalence of complete anosmia due to severely hypoplastic or (more usually) absent OBs. Therefore, loss of OB following kal shRNA-2 electroporation observed in *in situ* hybridisation and dose-relevant experiments

validates the specificity and efficiency of kal shRNA-2. We then consider loss of OB with stronger RFP expression as the indicator for kal knock down and performed the following histochemistry and immunofluorescence on the sections of both OB-present/absent forebrains from each embryo.

3.3 OEC defects in chick embryos with *kal* gene knock down

In chick, olfactory sensory neurons extend their axons towards the forebrain reaching the presumptive bulb region by stage 21 (E3.5). By stage 30 (E7) the bulb region begins to differentiate, acquiring its characteristic structure by stage 36 (E10) (Gomez and Celii, 2008). The H&E stained specimen of one side of the 2mg/ml kal shRNA-2 electroporated OB, revealed a distinct laminar organization at E10, including olfactory nerve, external plexiform, mitral cell, internal plexiform and granule cell layers (Fig. 3a and b). The connection of olfactory axons with this side of the OB was evident by βIII-tubulin immuno stained olfactory axons in the outmost ONL (Fig. 3c). On the contralateral presumptive OB with knock-down *kal*, there was no distinct laminar structure formation and there was a lack of olfactory axon connections with the forebrain. Notably, the bulk of the cell bodies of mitral cells form an irregular mass of cells (Fig. 3a2)， devoid of typical stratified structure seen in the normal side of OB (Fig. 3a1).

OECs are specialized glial cells involved in the growth and guidance of olfactory axons. They originate from the neural crest in mice and chicks and are heterogeneous in the pattern of markers they express in the PNS and CNS (Barraud et al., 2010; Forni et al., 2011; Katoh et al., 2011). SOX10, a marker of neural crest-derived OECs, is co-expressed with another OEC marker, BLBP, along the olfactory, vomeronasal, and terminal nerve pathways, in the frontonasal mesenchyme, and in the migratory mass and the OB in mouse (Pingault et al., 2013).

To examine the possibility that abnormal OB morphogenesis in *kal* knock down embryos might result from the OEC developmental defects, we immunostained sections of E10 embryos electroporated with scrambled and kal shRNA-2 with antibodies for SOX10 and BLBP. Consistent with previous reports (Barraud et al., 2013;Pingault et al., 2013), SOX10 and BLBP-expressing cells in scrambled control embryos were localised to the outermost layer of the OB, corresponding to the ONL. BLBP positive cells were rarely observed around the invading olfactory axons, being more densely expressed in ONL forming a much thicker layer (Fig. 4a). In contrast, SOX10 expressing cells were abundant in

olfactory axon bundles and formed a much thinner layer around the superficial surface of OB (Fig. 4b). We then determined the expression patterns of OEC markers in the presence of *kal* knock down. On the side of the morphologically normal OB, BLBP and SOX10 positive cells showed a similar expression profile to control embryos. By contrast, in the *kal* knockdown OB, BLBP expression appeared to incompletely encircle the surface of anterior forebrain, at the site of the OB anlage, forming a thinner and poorly organized layer (Fig. 4a). Strikingly, SOX10 expressing cells were completely absent in the anterior forebrain where there was no OB formation and lack of olfactory axonal connection (Fig. 4b). These observations imply that the chick *kal* product, anosmin, may be a determinant of differential OECs expression of SOX10 and BLBP. It is also possible that the survival and apoptosis of SOX10 and BLBP positive OECs might be directly or indirectly modulated by anosmin, especially for SOX10 expressing OECs.

GFAP, an astrocyte marker, is also expressed in more developmentally mature OECs in the middle-to-outer region of the ONL (Astic et al., 1998; Murthy et al., 2014; Raucci et al., 2013). To examine the role of anosmin-1 in OEC maturation, we further performed GFAP immunostaining on E10 forebrains electroporated with kal shRNA-2. GFAP expression was found to be weakly positive along the peripheral edge of the *kal* knock down forebrain, but negative on the contralateral side with normal OB (Fig. 4c). Taken together, these results support a potential role of anosmin-1 in determining the fate of OECs by preventing OECs from differentiating towards maturity.

3.4 Anosmin-1 inhibits OECs maturation in chick E10 OB explants.

As GFAP expression in the ONL is weak during early development stage (Astic et al., 1998), we further investigated the inhibitory capability of anosmin-1 on the maturation of immature OB glial cells in *ex vivo* explant cultures. We dissected E10 OB from the forebrain and embedded them in collagen gel. As seen in Fig. 5a and b, when OB explants (n=9) were placed in culture for 2 hours, no obvious GFAP-positive cells could be detected in all OB explants. After 3 days culture, in approximately 90% explants GFAP-positive cells were observed accumulating along the outermost ONL of the OB (n=15). Such a response is predominant in the anterior tip of OB at a site where incoming axons of olfactory sensory neurons normally penetrate, which is highly likely due to enhanced differentiation of immature OECs into mature GFAP+ OECs. Following 3 day anosmin-1 treatment, GFAP expression in ONL was dramatically reduced in 80% OB explants (n=20) (Fig. 5a and b, and

supplemental data 2 Fig. S1), demonstrating that anosmin-1 is able to inhibit OECs maturation.

3.5 Anosmin-1 inhibits GFAP expression in purified E10 OB immature glial cells

To further investigate the action of anosmin-1 on OEC maturation, we isolated OB glial cells from E10 chick embryos by differential attachment to a tissue culture flask. Enzymatically dissociated cells were shaken to remove neurons and microglia, and then glial differentiation induced by addition of medium with G5 supplement. As seen in Fig. 6a, purified OB cells expressed transitin (the avian homologue of nestin), vimentin and BLBP, but not other neuronal, oligodendrocyte and radial glia markers including Pax6, TuJ-1 and O4 (data not shown), indicating that they are immature OB glial cells, most likely a mixture of immature OEC subpopulations. With respect to three FGF receptors, the c isoforms of *fgfr* 1-3 and *fgfr* 1b, 3b isoforms were found to be expressed. These putative immature glial cells expressed *kal* (Fig. 6b), as shown by RT-PCR, but with very low or even no anosmin expression, which cannot be detected by immunocytochemistry and Western blotting using an antibody specific to chicken anosmin.

After 7 DIV, these OB immature glial cells began to express GFAP. GFAP-positive cells exhibited flat and multipolar morphology (Fig. 6c). Overexpression of chicken anosmin by the transfection of an anosmin expression construct demonstrated a more elongated morphology with less GFAP expression as compared with the empty vector control (Fig. 7a I). Moreover, Western blotting further showed that over-expression of chicken anosmin significantly reduced GFAP expression by approximately 50% (Fig. 7a II and III). Taken together, these data demonstrated that anosmin prevents OB immature glial cells from differentiating into a mature glial state.

We further examined the involvement of FGF signalling in mediating the actions of recombinant anosmin-1 in blocking OEC cell maturation. In Fig. 7b I and II, exogenous anosmin-1 maintained cells at 7 DIV with reduced GFAP expression by approximately 70%, which was reversed by the FGFR inhibitor Su5402 with cells presenting an elongated morphology. We also count the cells and found no effect of anosmin-1 on the cell numbers (data not shown). A similar effect to down-regulate GFAP expression by approximately 70% was seen with 2nM FGF2 treatment. Taken together, these data demonstrated a role of anosmin-1 on OB immature glial cell differentiation via FGF signalling, inhibiting differentiation into the mature glial cells by promoting FGF signalling.

4 DISCUSSION

Since *KAL-1* is absent in the genomes of mouse and rat, other vertebrate species have been employed to investigate the biology of anosmin-1 during development. As previously revealed in zebrafish, anosmin-1 influences fasciculation and terminal targeting of olfactory axons into the OB (Yanicostas et al., 2009). This might be the direct effect of anosmin-1 on axonal outgrowth and targeting or the secondary effect on OEC differentiation and maturation for de-fasciculation and synaptogenesis inside the OB. Our chick model using *in ovo* electroporation to knock down *kal* shows that loss of function of anosmin results in abnormal OEC maturation, suggesting a novel mechanism whereby anosmin-1 modulates OEC development during olfactory system ontogeny.

Loss-of-function mutations in SOX10 have been found in KS patients with hearing impairment (Barnett et al., 2009;Finzsch et al., 2010;Pingault et al., 2013). SOX10, a member of high mobility group domain-containing transcription factors, has recently been found to be associated with olfactory development. In SOX10 deleted mice, expression of the early glial differentiation marker BLBP was significantly decreased in the outmost ONL (Pingault et al., 2013), consistent with our observations that *kal* depleted chick embryos showed thinner BLBP layer with complete absence of SOX10 in the ONL. We also observed GFAP expression in the ONL at E10, at a much earlier stage than normal GFAP expression when chick anosmin was down-regulated. This sort of GFAP up-regulation might be accompanied by decreased expression of SOX10 as evidenced in p75-deleted mice that these two OEC markers are expressed in an inverse manner (Raucci et al., 2013). Furthermore, it has been reported that mouse OECs are GFAP positive at E15 in the olfactory axon fascicles, but negative in the ONL until E18.5 with persistent weak expression until P20 (Astic et al., 1998). However, significantly higher *kal* expression occurs in chick OB from E10 to newly hatched chick (21 days) followed by progressively reduced expression in adulthood (Rugarli et al., 1993); such an expression profile is inversely correlated with GFAP, further reinforcing the fundamental regulatory role of anosmin-1 in delaying OECs maturation from immature SOX10 and BLBP expressing cells.

Disrupted balance between SOX10/BLBP+ immature OEC and GFAP+ mature OEC populations in the absence of anosmin-1 is thought to be associated with abnormal OB development. In SOX10 null mice, OBs were morphologically well-formed and innervated by incoming olfactory axons, in contrast to the situation in the current study in which the OBs were completely lost in the absence of anosmin action. One explanation is that anosmin-1

might regulate other SOX family proteins in additional to SOX10, affecting multi-functional activities between SOX proteins as reported for SOX10 on vagal neural crest cells and various other neural crest cell derivatives (Paratore et al., 2001; Southard-Smith et al., 1998). It is also possible that anosmin-1 might determine the differentiation of multiple subpopulations of immature OECs other than SOX10+ OECs only. The fact that BLBP+ OEC layer in anosmin-depleted OBs turned to be dramatically thinner supports this possibility. Another possibility is an unexpected upregulation of GFAP in OECs between E8 and E10 when chick olfactory axons connect to the OBs. It has been shown that the magnitude of GFAP expression in astrocytes is associated with the stiffness of intermediate filaments (Duffy et al., 1982). Premature maturation of OECs might lead to loss of immature OEC phenotype of shape, motility and flexibility which facilitate olfactory axonal sorting and specific synapse formation in OBs; this would result in lack of OB cell differentiation required for normal OB morphogenesis. Finally, H&E stained sections showed that there is an irregular mass of mitral cells in the *kal* knock-down E10 OBs without the typical formation of the stratified structure (Fig. 3a1 and a2), possibly altering the environment for OEC maturation, innervation and targeting in ONL.

In chick, transient expression of *kal* was first observed at the early HH5+ to HH9 developmental stages, when the cranial neural crest is formed; the expression level progressively decreases during or after the time of neural crest cell migration at HH9 (Endo et al., 2012). As SOX10 positive OECs originate from neural crest, it is possible that anosmin-1 plays a role in OEC specification during gastrulation. In the present study, we electroporated chick embryos at HH 11–12 (E2), prior to the developmental window for initial OEC fate specification in the neural crest, and then focused on OEC development in the OB at E10; we are therefore not able to give a clear answer to this question as to whether anosmin-1 is involved in OEC fate determination inside neural crest.

OECs stimulate axon growth during development and promote plasticity of spared fibres when implanted into injured CNS (Raisman and Li, 2007; Tennent and Chuah, 1996); these properties make them an attractive cell type for cell-based treatment of neuronal regeneration after CNS injury (Gómez et al., 2018). Different subpopulations of OECs are believed to perform distinct subtype-specific functions (Honore et al., 2012; Ubink and Hokfelt, 2000). One of the interesting properties of OECs is their interaction with astrocytes, preventing reactive astrocytosis and glial scar formation after their implantation at a CNS lesion site (Lakatos et al., 2000; Lakatos et al., 2003; Santos-Silva et al., 2007). These actions

are likely to be mediated by immature OECs. It has been suggested that FGF signalling via an FGF2/FGFR1/HS pathway underlies the molecular regulation of OECs/astrocyte interaction (Higginson et al., 2012; Santos-Silva et al., 2007). We have previously proposed a mechanism whereby anosmin-1 has a dual role on the assembly and activation of the FGF2/FGFR1/HS complex (Hu et al., 2009). Our present results might support a potential role of anosmin-1 as a candidate molecule in preserving OECs in an immature state to minimize astrocyte activation for the incoming or regenerative axons navigating through an astroglial barrier.

Anosmin-1 is not sufficient by itself to induce proper OB formation as evidenced by the fact that ablation of chick olfactory placode resulted in histologically abnormal OB where anosmin-1 was still expressed at high levels (Lutz et al., 1994). In anosmin-1 mutated human KS foetuses and FGFR1-deficient mice, neurogenesis of olfactory neurons appears to be preserved (Hebert et al., 2003; Schwanzel-Fukuda et al., 1989; Teixeira et al., 2010). This implies that the main consequences of anosmin-1/FGF signalling lie within the domain of glia development/interaction, especially modifying OECs maturation. Our studies enable us to propose a model whereby, during OB development, loss of function of anosmin-1 on FGF signalling regulation disrupts OEC maturation/differentiation, thereby interfering with olfactory axons from targeting and penetrating into the forebrain (Fig. 8).

Acknowledgments: This work was supported by National Natural Science Foundation of China (NSFC) (81571193)

Conflict of interest: The authors declare no conflict of interest.

Data Accessibility： Dataset: Hu, Youli, 2019, "Replication Data for", https://doi.org/10.7910/DVN/SKFGBT, Harvard Dataverse, DRAFT VERSION

Abbreviations

ABM: DMEM/F12 medium

AGM: ABM with 10% (v/v) fetal bovine serum

DIV: days *in vitro*

E: embryonic day

FBS: fetal bovine serum

GnRH: gonadotropin-releasing hormone

H&E: haemotoxylin and eosin

HH stage: Hamburger–Hamilton stage

KS: Kallmann syndrome

OECs: Olfactory ensheathing cells

OB: olfactory bulb

ONL: olfactory nerve layer

PFA: paraformaldehyde in PBS

References

Astic L, Pellier-Monnin V, Godinot F. (1998) Spatio-temporal patterns of ensheathing cell differentiation in the rat olfactory system during development. *Neuroscience* **84**:295-307.

Barnett CP, Mendoza-Londono R, Blaser S, Gillis J, Dupuis L, Levin AV, Chiang PW, Spector E, Reardon W. (2009) Aplasia of cochlear nerves and olfactory bulbs in association with SOX10 mutation. *Am J Med Genet A* **149A**:431-436.

Barraud P, Seferiadis AA, Tyson LD, Zwart MF, Szabo-Rogers HL, Ruhrberg C, Liu KJ, Baker CV. (2010) Neural crest origin of olfactory ensheathing glia. *Proc Natl Acad Sci U S A* **107**:21040-21045.

Barraud P, St John JA, Stolt CC, Wegner M, Baker CV (2013) Olfactory ensheathing glia are required for embryonic olfactory axon targeting and the migration of gonadotropin-releasing hormone neurons. *Biol Open* **2**:750-759.

Doucette R. (1991) PNS-CNS transitional zone of the first cranial nerve. *J Comp Neurol* **312**:451-466.

Duffy PE, Huang YY, Rapport MM. (1982) The relationship of glial fibrillary acidic protein to the shape,motility, and differentiation of human astrocytoma cells. *Exp Cell Res* **139**:145-157.

Endo Y, Ishiwata-Endo H, Yamada KM. (2012) Extracellular matrix protein anosmin promotes neural crest formation and regulates FGF, BMP, and WNT activities. *Dev Cell* **23**:305-316.

Farbman AI. (1990) Olfactory neurogenesis: genetic or environmental controls? *Trends Neurosci* **13**:362-365.

Finzsch M, Schreiner S, Kichko T, Reeh P, Tamm ER, Bosl MR, Meijer D, Wegner M. (2010) Sox10 is required for Schwann cell identity and progression beyond the immature Schwann cell stage. *J Cell Biol* **189**:701-712.

Forni PE, Taylor-Burds C, Melvin VS, Williams T, Wray S. (2011) Neural crest and ectodermal cells intermix in the nasal placode to give rise to GnRH-1 neurons, sensory neurons, and olfactory ensheathing cells. *J Neurosci* **31**:6915-6927.

Geller S, Lomet D, Caraty A, Tillet Y, Duittoz A, Vaudin P. (2017) Rostral-caudal maturation of glial cells in the accessory olfactory system during development: involvement in outgrowth of GnRH neuritis. *Eur J Neurosci* **46**:2596-2607

Gomez G, Celii A. (2008) The peripheral olfactory system of the domestic chicken: physiology and development. *Brain Res Bull* **76**:208-216.

Gómez RM, Sánchez MY, Portela-Lomba M, Ghotme K, Barreto GE, Sierra J, Moreno-Flores MT. (2018). Cell therapy for spinal cord injury with olfactory ensheathing glia cells (OECs). *Glia* **Jan 13**. doi: 10.1002/glia.23282.

Gonzalez-Martinez D, Kim SH, Hu Y, Guimond S, Schofield J, Winyard P, Vannelli GB, Turnbull J, Bouloux PM. (2004) Anosmin-1 modulates fibroblast growth factor receptor 1 signaling in human gonadotropin-releasing hormone olfactory neuroblasts through a heparan sulfate-dependent mechanism. *J Neurosci* **24**:10384-10392.

Graziadei GA& Graziadei PP. (1979) Neurogenesis and neuron regeneration in the olfactory system of mammals. II. Degeneration and reconstitution of the olfactory sensory neurons after axotomy. *J Neurocytol* **8**:197-213.

Hebert JM, Lin M, Partanen J, Rossant J, McConnell SK. (2003) FGF signaling through FGFR1 is required for olfactory bulb morphogenesis. *Development* **130**:1101-1111.

Higginson JR, Thompson SM, Santos-Silva A, Guimond SE, Turnbull JE, Barnett SC. (2012)

Differential sulfation remodelling of heparan sulfate by extracellular 6-O-sulfatases regulates fibroblast growth factor-induced boundary formation by glial cells: implications for glial cell transplantation. *J Neurosci* **32**:15902-15912.

Honore A, Le CS, Derambure C, Normand R, Duclos C, Boyer O, Marie JP, Guerout N. (2012) Isolation, characterization, and genetic profiling of subpopulations of olfactory ensheathing cells from the olfactory bulb. *Glia* **60**:404-413.

Hu Y, Gonzalez-Martinez D, Kim SH, Bouloux PM. (2004) Cross-talk of anosmin-1, the protein implicated in X-linked Kallmann's syndrome, with heparan sulphate and urokinase-type plasminogen activator. *Biochem J* **384**:495-505.

Hu Y, Guimond SE, Travers P, Cadman S, Hohenester E, Turnbull JE, Kim SH, Bouloux PM. (2009) Novel mechanisms of fibroblast growth factor receptor 1 regulation by extracellular matrix protein anosmin-1. *J Biol Chem* **284**:29905-29920.

Katoh H, Shibata S, Fukuda K, Sato M, Satoh E, Nagoshi N, Minematsu T, Matsuzaki Y, Akazawa C, Toyama Y, Nakamura M, Okano H. (2011) The dual origin of the peripheral olfactory system: placode and neural crest. *Mol Brain* **4**:34.

Lakatos A, Barnett SC, Franklin RJ. (2003) Olfactory ensheathing cells induce less host astrocyte response and chondroitin sulphate proteoglycan expression than Schwann cells following transplantation into adult CNS white matter. Exp Neurol **184**:237-246.

Lakatos A, Franklin RJ, Barnett SC. (2000) Olfactory ensheathing cells and Schwann cells differ in their in vitro interactions with astrocytes. *Glia* **32**:214-225.

Legouis R, Lievre CA, Leibovici M, Lapointe F, Petit C (1993) Expression of the KAL gene in multiple neuronal sites during chicken development. Proc Natl Acad Sci U S A 90:2461-2465.

Li Y, Field PM, Raisman G. (2005) Olfactory ensheathing cells and olfactory nerve fibroblasts maintain continuous open channels for regrowth of olfactory nerve fibres. *Glia* **52**:245-251.

Lutz B, Kuratani S, Rugarli EI, Wawersik S, Wong C, Bieber FR, Ballabio A, Eichele G. (1994) Expression of the Kallmann syndrome gene in human fetal brain and in the manipulated chick embryo. *Hum Mol Genet* **3**:1717-1723.

Murthy M, Bocking S, Verginelli F, Stifani S. (2014) Transcription factor Runx1 inhibits proliferation and promotes developmental maturation in a selected population of inner olfactory nerve layer olfactory ensheathing cells. *Gene* **540**:191-200.

Nieto MA, Patel K, Wilkinson DG. (1996) In situ hybridization analysis of chick embryos in whole mount and tissue sections. *Methods Cell Biol* **51**:219-235.

Paratore C, Goerich DE, Suter U, Wegner M, Sommer L. (2001) Survival and glial fate acquisition of neural crest cells are regulated by an interplay between the transcription factor Sox10 and extrinsic combinatorial signaling. *Development* **128**:3949-3961.

Pingault V, Bodereau V, Baral V, Marcos S, Watanabe Y, Chaoui A, Fouveaut C, Leroy C, Verier-Mine O, Francannet C, Dupin-Deguine D, Archambeaud F, Kurtz FJ, Young J, Bertherat J, Marlin S, Goossens M, Hardelin JP, Dode C, Bondurand N. (2013) Loss-of-function mutations in SOX10 cause Kallmann syndrome with deafness. *Am J Hum Genet* **92**:707-724.

Raisman G. (1985) Specialized neuroglial arrangement may explain the capacity of vomeronasal axons to reinnervate central neurons. *Neuroscience* **14**:237-254.

Raisman G & Li Y. (2007) Repair of neural pathways by olfactory ensheathing cells. *Nat Rev Neurosci* **8**:312-319.

Raucci F, Tiong JD, Wray S (2013) P75 nerve growth factor receptors modulate development of GnRH neurons and olfactory ensheating cells. *Front Neurosci* **7**:262.

Rugarli EI, Lutz B, Kuratani SC, Wawersik S, Borsani G, Ballabio A, Eichele G. (1993)

Expression pattern of the Kallmann syndrome gene in the olfactory system suggests a role in neuronal targeting. *Nat Genet* **4**:19-26.

Santos-Silva A, Fairless R, Frame MC, Montague P, Smith GM, Toft A, Riddell JS, Barnett SC. (2007) FGF/heparin differentially regulates Schwann cell and olfactory ensheathing cell interactions with astrocytes: a role in astrocytosis. *J Neurosci* **27**:7154-7167.

Schwanzel-Fukuda M, Bick D, Pfaff DW. (1989) Luteinizing hormone-releasing hormone (LHRH)-expressing cells do not migrate normally in an inherited hypogonadal (Kallmann) syndrome. *Brain Res Mol Brain Res* **6**:311-326.

Schwob JE (2002) Neural regeneration and the peripheral olfactory system. *Anat Rec* **269**:33-49.

Soussi-Yanicostas N, Faivre-Sarrailh C, Hardelin JP, Levilliers J, Rougon G, Petit C. (1998) Anosmin-1 underlying the X chromosome-linked Kallmann syndrome is an adhesion molecule that can modulate neurite growth in a cell-type specific manner. *J Cell Sci* **111** (Pt 19):2953-2965.

Southard-Smith EM, Kos L, Pavan WJ. (1998) Sox10 mutation disrupts neural crest development in Dom Hirschsprung mouse model. *Nat Genet* **18**:60-64.

Teixeira L, Guimiot F, Dode C, Fallet-Bianco C, Millar RP, Delezoide AL, Hardelin JP. (2010) Defective migration of neuroendocrine GnRH cells in human arrhinencephalic conditions. *J Clin Invest* **120**:3668-3672.

Tennent R, Chuah MI (1996) Ultrastructural study of ensheathing cells in early development of olfactory axons. Brain Res Dev Brain Res 95:135-139.

Ubink R & Hokfelt T. (2000) Expression of neuropeptide Y in olfactory ensheathing cells during prenatal development. *J Comp Neurol* **423**:13-25.

Williams SK, Franklin RJ, Barnett SC. (2004) Response of olfactory ensheathing cells to the degeneration and regeneration of the peripheral olfactory system and the involvement of the neuregulins. *J Comp Neurol* **470**:50-62.

Yanicostas C, Herbomel E, Dipietromaria A, Soussi-Yanicostas N. (2009) Anosmin-1a is required for fasciculation and terminal targeting of olfactory sensory neuron axons in the zebrafish olfactory system. *Mol Cell Endocrinol*. **312**:53-60.

Figure 1. Silencing efficiency of kal shRNA on *kal* gene expression. (a) CHO cells were co-transfected with a chick 6xHis tagged anosmin-1 expression construct (*kal* in pCAGGS) without (-) or with empty vector, scrambled shRNA and three kal shRNAs (1-3), cultured for 2 days and then processed for immunoblotting using anosmin-1 antibody, using β-actin antibody as loading control. kal shRNA-2 generated optimal silencing on anosmin-1 expression and was subsequently used for *in ovo* electroporation on chick embryos. (b) Chick E2 embryos were electroporated with 2mg/ml shRNAs including vector only (-) (n=6), scrambed shRNA (n=6) or kal siRNA-2 (n=3). After incubation to E10 stage, the embryos were dissected, fixed and processed for *in situ* hybridization with anti-sense *kal* probe; sense *kal* probe was used as negative control. In vector only (-) embryo forebrains (I), the *kal* expression was present in the normal OBs with anti-sense *kal* probe, but absent with sense *kal* probe (II). Low magnification images are on the left side and high magnification images on the right side. (III) In scrambed shRNA embryo forebrains, the *kal* expression was present in both normal OBs with anti-sense *kal* probe. Low magnification images are on the left side and high magnification images on the right side. (IV) For kal shRNA-2 electroporation, left side image is low magnification showing normal and abnormal OB from one electroporated embryos. The normal OB with *kal* expression developed well on one side of forebrain, while on the contralateral side of forebrain without *kal* expression, OB was absent. Their higher magnification images are on the middle and right side respectively. Representative images from embryo forebrains in each group are shown. Scale bar: low magnification image, 100μm; high magnification image, 20μm. F: forebrain; single arrow: normal OB; double arrow: absent OB.

Figure 2. Dose-relevant effect of kal shRNA-2 on OB development of E10 chick embryos. E2 chick embryos were electroporated with 2mg/ml srcambled shRNA (a) and kal shRNA-2 at 0.8 (b), 2mg/ml (c) respectively, incubated for 8 days to E10 stage, and dissected for visualisation under epifluorescence microscopy. (a) and (b) Both OBs developed normally with scrambled shRNA and lower kal shRNA-2 concentration even in the OBs with higher RFP expression (n=8 embryos, for each group from two independent experiments). (c) Higher concentration of kal shRNA-2 at 2mg/ml resulted in very small or no OBs and the lack of penetration of olfactory sensory axon bundles in one side of forebrain with much higher RFP expression. The contralateral side with less RFP showed normal OB formation and normal connection of axon bundles to the OB. Four embryos electroporated with 2mg/ml

kal shRNA-2 are represented from two experiments (n=10). Upper panel: bright field image; lower panel: fluorescent image. Scale bar: 20μm. F: forebrain; n′ : axon bundles of olfactory sensory neurons; arrow: normal OB; asterisk: abnormal OB.

Figure 3. Morphological defects of E10 chick OBs electroporated with 2mg/ml kal shRNA-2. E2 chick embryos were electroporated with 2mg/ml kal shRNA-2, incubated to E10, fixed and paraffin sectioned for H&E (a,b) and βIII-tubulin immunostaining (c). (a) H&E staining revealed normal OB morphology with distinct lamination from outside to inside: olfactory nerve layer (ONL), external plexiform layer (EPL), mitral cell layer (ML), internal plexiform layer (IPL) and granule cell layer (GL). By contrast, on the *kal* knock down side of forebrain, there was no obvious typical laminar structure formation. (b) H&E staining on a deeper section. Similar morphological defects of OBs were observed on different sections, demonstrating that such defects are not due to the orientation during sectioning. (a1) and (a2): the higher magnification of the boxed regions in (a). (c) Section was immunostained with βIII-tubulin antibody (red) and counterstained with Hoechst (blue). Olfactory sensory axons were present in the ONL of OB (white arrows), but absent on the *kal* knock down side of the forebrain. The higher magnification of the boxed region is shown in (c1). Representative images show staining on the sections of three OBs (n=3) under each of the stated conditions. Scale bar: (a) and (b), 100μm; other images, 20μm. F: forebrain; black arrow: normal OB; asterisk: abnormal OB.

Figure 4. OEC defects in chick OBs electroporated with 2mg/ml kal shRNA-2. (a and b) E2 chick embryos were electroporated with 2mg/ml scrambled shRNA and kal shRNA-2, cultured to E10, dissected and cryostat sectioned for immunostaining with antibodies against OEC markers BLBP (a) and SOX10 (b) (top panel). Middle panel: Hoechst nuclear staining. Bottom panel: the higher magnification of the boxed regions in the (a), (b) and (b3). (c) E2 chick embryos were electroporated with 2mg/ml kal shRNA-2, cultured to E10 stage. The cryostat sections were then immunostained with antibody to GFAP (green) and counterstained with Hoechst (blue). GFAP expression was positive along the peripheral edges of *kal* knock down side of anterior forebrain, but negative on the contralateral side. (c1) is the higher magnification of the boxed regions in (c). Representative images show immunostaining on the sections of the OBs (n=3) in each group. Scale bar: (a), (b) and (c),

100μm; (a1-2), (b1-3) and (c1), 20 μm. F: forebrain; white arrow: normal OB; asterisk: absent OB.

Figure 5. Anosmin-1 inhibits OECs maturation in chick E10 OB explants. Intact E10 OBs in collagen gel were cultured for 2h or 3 DIV with or without 5nM recombinant anosmin-1, either fixed directly (a) or cryostat sectioned (b), followed by immunohistochemical staining with GFAP antibody. (a) Representative images from OB explants in three independent experiments of each group (n=9, 15 and 20 respectively) are shown. (b) Representative images show immunostaining on the sections of the OBs (n=3) in each group. top panel: bright field; middle panel: low magnification, scale bar: 100μm; bottom panel: high magnification of anterior tip of OB, scale bar: 20μm. White dotted line indicates the penetration site of olfactory sensory axons into the OB.

Figure 6. Primary culture of purified OB immature glial cells. (a) E10 OB cells were dissociated with trypsin, cultured in media containing 10% (v/v) serum for two weeks, followed by shaking to remove neurons and microglia, and cultured in glial serum-free differentiation medium with G5 supplement. OB cells were immunostained with antibodies for transitin, vimentin and BLBP. (b) RT-PCR was performed with specific primers for *fgfr1-3* b and c isoforms and *kal*. (c) OB immature glial cells were immunostained with GFAP antibody after 1 DIV and 7 DIV culture. Cells were GFAP-positive after 7 DIV, exhibiting flat and polygonal morphology.

Figure 7. Anosmin-1 prevents OB immature glial cells from differentiating into a mature state via FGF signalling. (a) OB immature glial cells were transfected with chicken anosmin expression vector and empty vector. OB immature glial cells with chicken anosmin overexpression demonstrated a more elongated morphology shown by immunocytochemistry (I) and diminished GFAP expression by western blot (II). Representative blots from three independent experiments are shown. (III) The relative band intensities were calculated and expressed as the relative GFAP to actin ratio and then compared with the control sample (vector only, 100%). *, $P<0.05$. (b) (I) OB immature glial cells were cultured in differentiation medium and treated with 5nM anosmin-1, 2nm FGF2, 5nM anosmin-1 plus 20μM FGFR1 inhibitor Su5402 for 7 DIV. Anosmin-1 and FGF2 reduced GFAP expression. FGFR1 inhibitor, Su5402, reversed anosmin-1 induced GFAP expression. Representative figures are from three independent experiments. Scale bar: 20 μm. (II) The fluorescence

intensities of GFAP expression were calculated and compared with the control sample (100%). **, P<0.01.

Figure 8. A model proposed for anosmin-1 regulation on OEC maturation via FGF signalling for OB development. (a) During OB development, SOX10+ and BLBP+ OECs, after birth in the neural crest, wrap olfactory sensory axons migrating towards the anterior forebrain where they, along with olfactory axons, form the ONL of OB. Anosmin-1 keeps SOX10+ and BLBP+ OECs in an immature state to assist olfactory axon targeting, penetration, defasiculation and synapse formation inside the OB, subsequently inducing OB morphogenesis. (b) Loss of function of anosmin-1 observed in X-KS embryos on FGF signalling regulation appears to cause OEC maturation/differentiation into GFAP + cells, thereby preventing olfactory axons forming stable connections with the forebrain. CP: cribriform plate; F: forebrain; OB: olfactory bulb; OE: olfactory epithelium; ORN: olfactory receptor neuron.

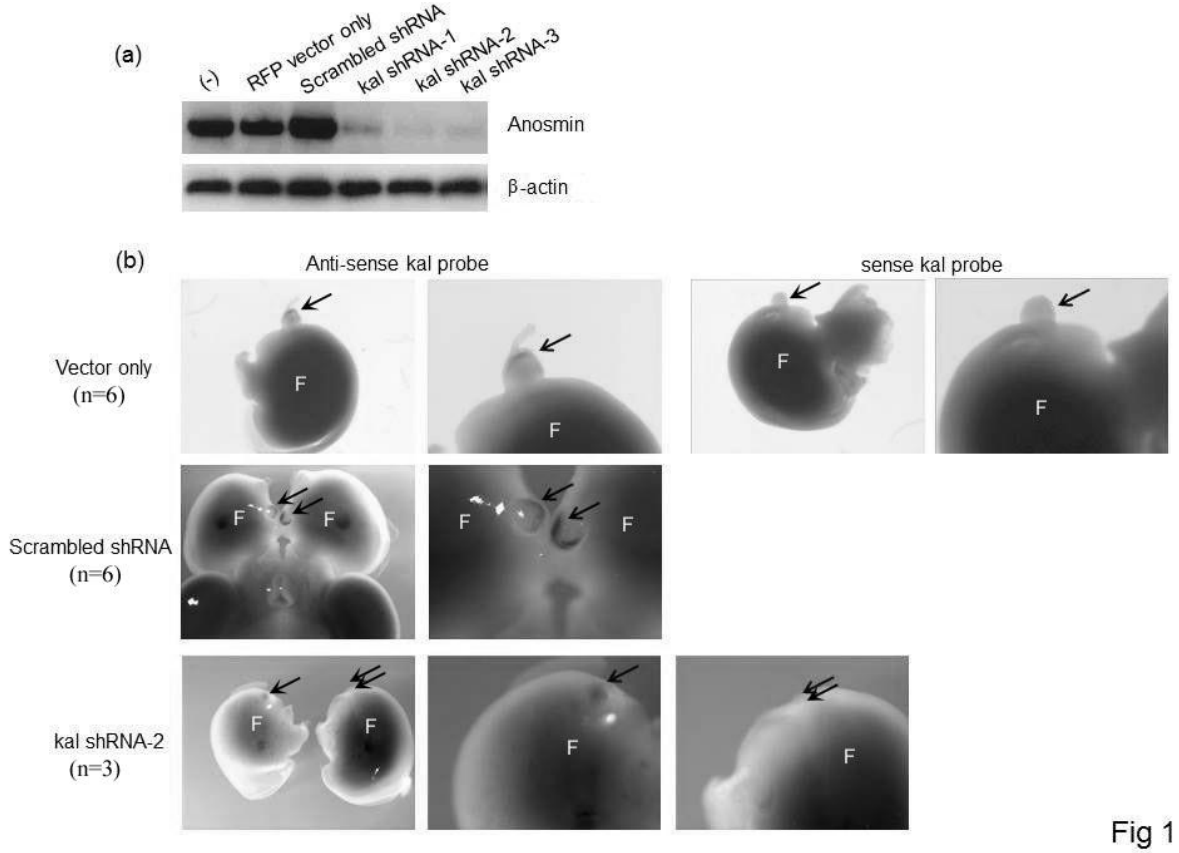

Fig 1

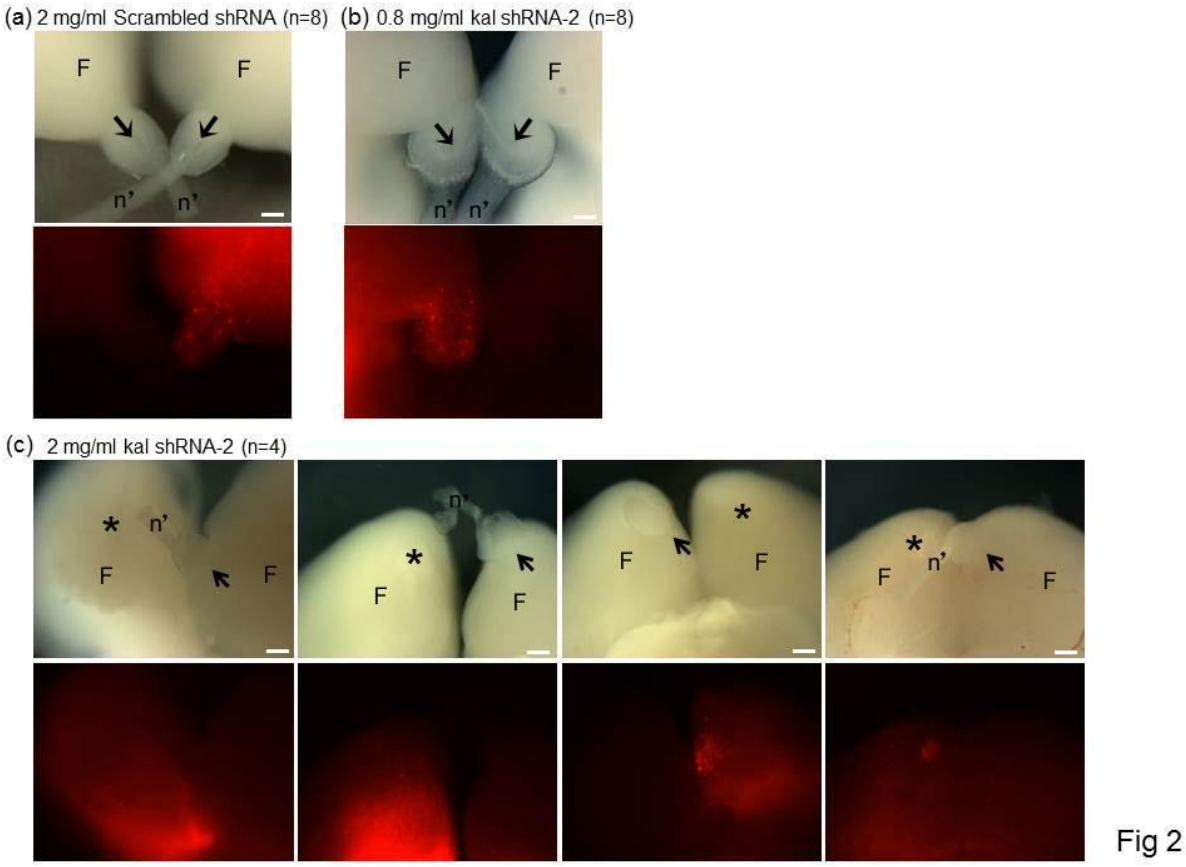

Fig 2

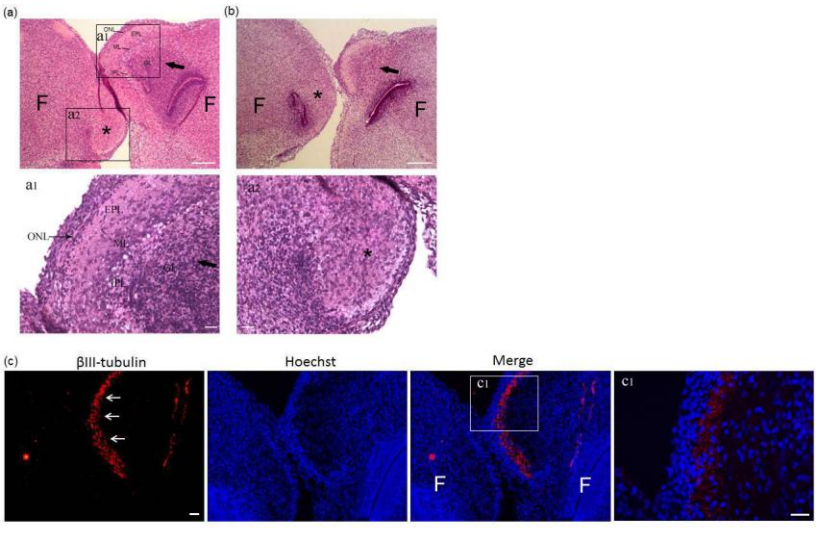

Fig 3

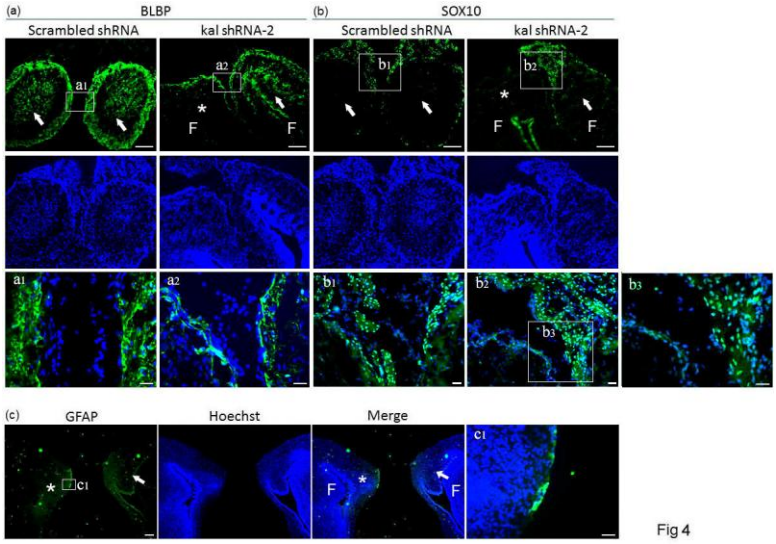

Fig 4

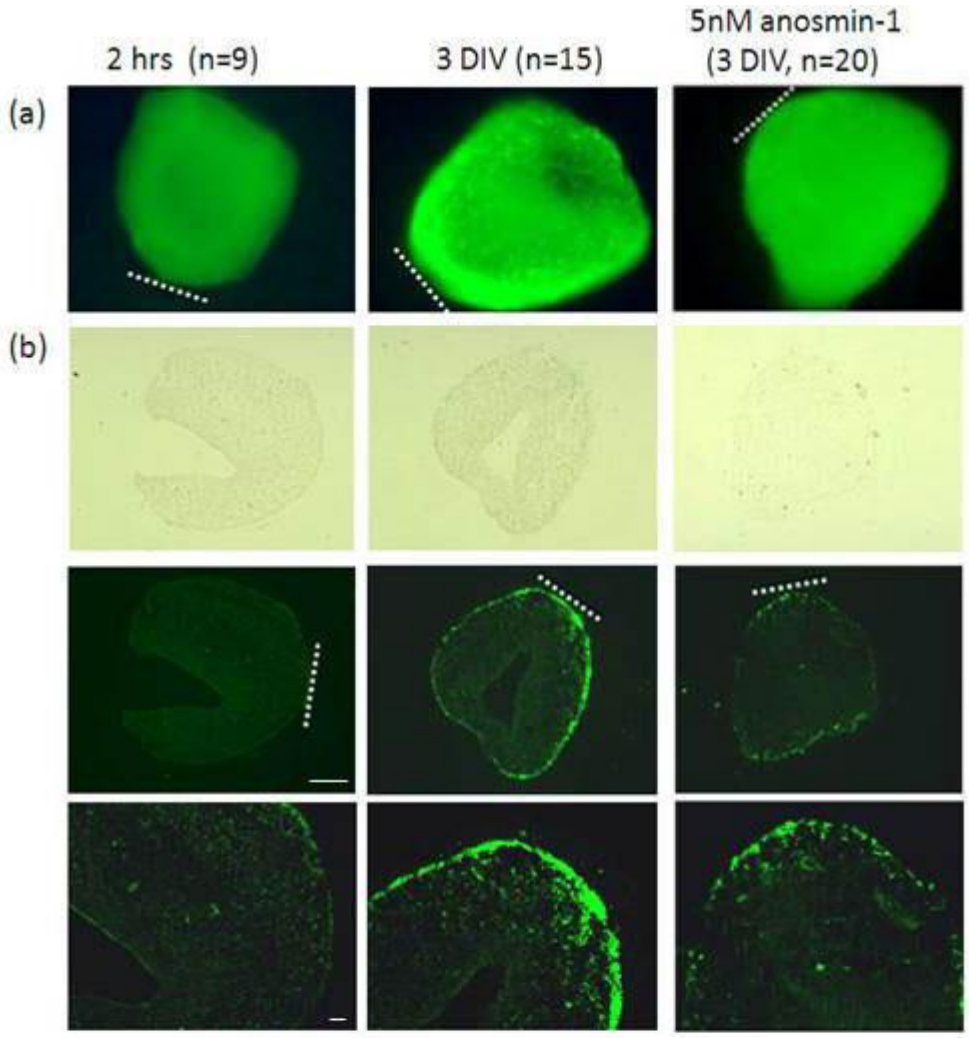

Fig 5

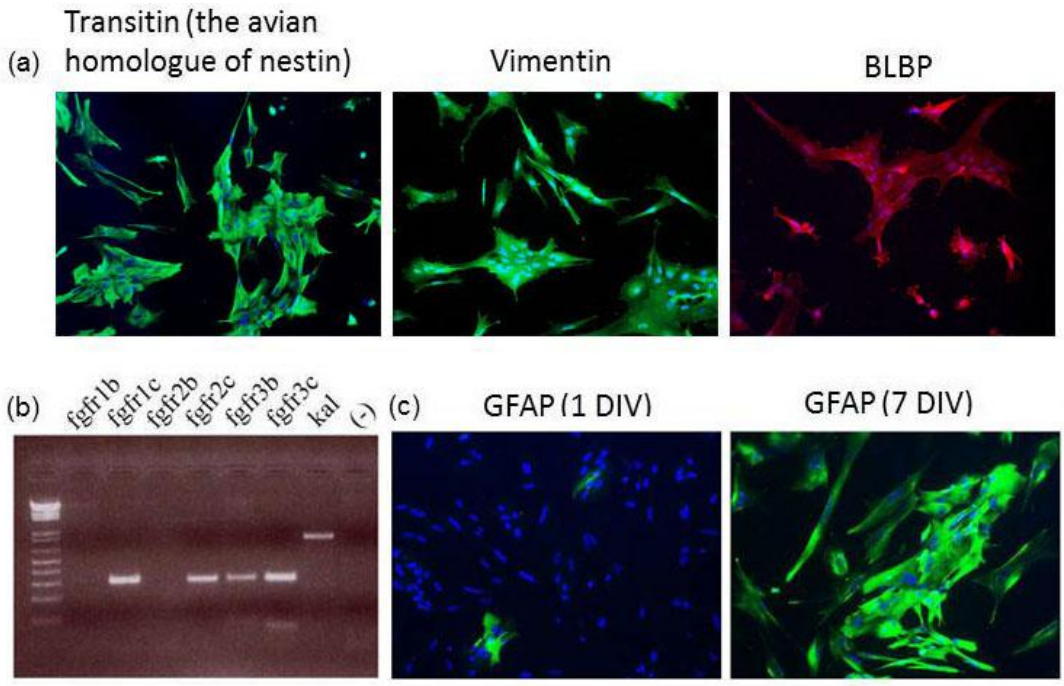

Fig 6

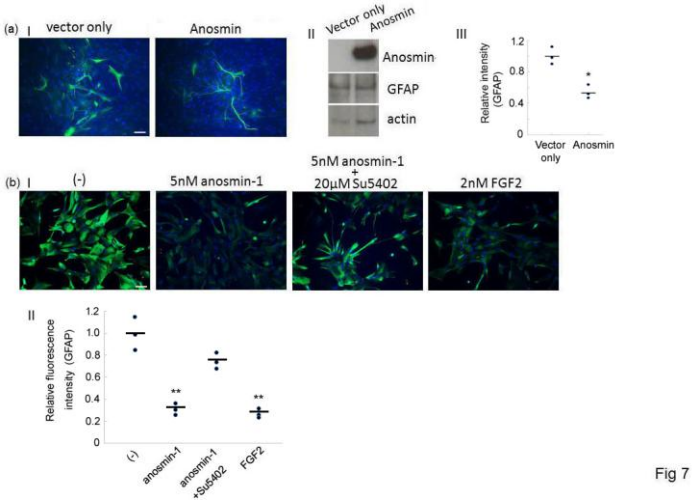

Fig 7

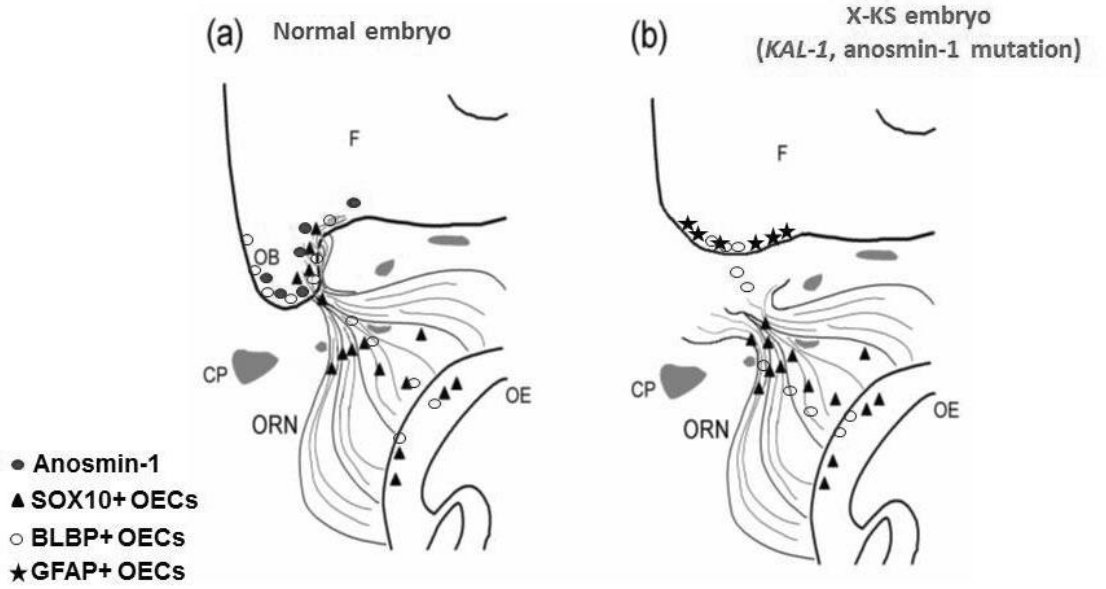

Fig 8